Solid−Liquid Equilibria in an L-Isoleucine + L-Alanine + Water System

Toshimichi Kamei,*,† Kazuhiro Hasegawa,† Tatsuki Kashiwagi,‡ Eiichiro Suzuki,‡ Masaaki Yokota,§ Norihito Doki,§ and Kenji Shimizu§

Isolation and Purification Technology Laboratory, Fermentation and Biotechnology Laboratories, Ajinomoto Co. Inc., 1-1 Suzuki-cho, Kawasaki-ku, Kawasaki-shi, 210-8681 Japan, Institute of Life Sciences, Ajinomoto Co., Inc., 1-1 Suzuki-cho, Kawasaki-ku, Kawasaki-shi, 210-8681 Japan, and Department of Chemical Engineering, Iwate University, 4-3-5 Ueda, Morioka, 020-8551 Japan

Solid−liquid equilibria in L-isoleucine (L-Ile) + L-alanine (L-Ala) and water were measured at 293 K using the crystallization method. The L-Ile solubility decreased gradually with increased mole fraction of L-Ala. However, the L-Ala solubility was not affected by the presence of a small amount of L-Ile. Regarding the solid phase, the formation of a solid solution of L-Ile and L-Ala was confirmed when solid phases contain much L-Ile. In contrast, only L-Ala crystallized when L-Ala and a small amount of L-Ile were in the liquid phase.

Introduction

We have been studying the batch crystallization of blanched chain amino acids.[1−3] As described in our previous work,[3] it is necessary to obtain fundamental data such as solid−liquid equilibria in aqueous amino acid systems to design the crystallization process of blanched chain amino acids.

In prior studies, solid−liquid equilibria in L-leucine (L-Leu) + L-valine (L-Val) and water and L-isoleucine (L-Ile) + L-valine (L-Val) and water were measured at 298 K using the crystallization method described by Kurosawa et al.[4,5] Kurosawa et al. provided evidence for the formation of solid solutions in their studies. They found that some peaks in the powder X-ray diffraction (XRD) pattern of crystals grown from aqueous solutions of the two amino acids could not be obtained by superposing the peaks in the diffraction patterns of crystals grown from binary with aqueous of the individual amino acids.[4,5] In addition, in our previous work,[3] solid−liquid equilibria in L-isoleucine (L-Ile) + L-norleucine (L-Nle) and water were measured at 293 K using the same crystallization method conducted by Kurosawa et al.,[4,5] and the formation of a solid solution was also confirmed. In these cases, the crystal structures of two amino acids are similar; the lattice constants are almost the same, except for the *c*-axis. The lattice constant and the system of L-Ile, L-Val, L-Leu, and L-Nle are presented in Table 1.[6−10]

Therefore, in the present study, solid−liquid equilibria in two amino acids with different crystal structures and water system were obtained, and the solid phase was confirmed. The L-isoleucine (L-Ile) + L-alanine (L-Ala) and water system was chosen as a representative case. The lattice constant and the system of L-Ala are also presented in Table 1.[6−10] Molecular structures of these amino acids are presented in Figure 1.

Experimental Section

Chemicals. The L-Ile and L-Ala used in this experiment were obtained commercially (pharmaceutical grade, 99.0 %) from Ajinomoto Co., Inc. (Tokyo, Japan). Acetone used in this experiment was a special grade chemical (99.5 % (GC)) from Junsei Chemical Co., Ltd. The water used in this experiment (specific resistivity, 18.2 MΩ·cm^{-1}; TOC, 4 ppb) was produced using a Milli-Q (Millipore Corp.) device.

Table 1. Unit Cell Constants and Systems from Single-Crystal XRD Data[6−10]

amino acid	system	lattice constant/Å		
		a	*b*	*c*
L-valine (L-Val)	monoclinic	9.71	5.27	12.06
L-leucine (L-Leu)	monoclinic	9.61	5.31	14.72
L-isoleucine (L-Ile)	monoclinic	9.75	5.32	14.12
L-norleucine (L-Nle)	monoclinic	9.55	5.26	15.38
L-alanine (L-Ala)	orthorombic	6.03	12.35	5.78

Procedure. The crystallization method was chosen for this experiment to confirm the solid−liquid equilibrium. It was the same way as those made by Kamei et al.[3] The scheme and experimental apparatus are presented in Figures 2a and 2b.

First, solid L-Ile and L-Ala were added to the water at room temperature. Then, the mixture of L-Ile, L-Ala, and water was heated to 80 °C and maintained at that temperature until the solution was dissolved completely. The compositions of the starting solutions are presented in Table 2. After dissolution, the solution was placed in a jacketed glass vessel, and then the vessel was sealed. The temperature was controlled to (80 ± 0.1) °C using circulating water in the jacket from a programmable water bath. Subsequently, the solution was concentrated in a vacuum at 50 °C and crystallized. After concentration, the concentrated slurry in the jacketed vessel was cooled rapidly to 20 °C using circulating water in the jacket. The cooling rate was 15 °C·h^{-1}. The temperature was then kept constant at 20 °C until no changes were observed in the liquid phase concentration. After achievement of steady state conditions, the vessel contents were filtered under a vacuum to collect the solid phase. After filtration, the obtained crystals were washed with 10 times the mass of acetone to remove adhesive impurities from the crystal surface. For example, if the weight of the wet crystal was 5 g, 50 g of acetone was used. Finally, crystals were dried at room temperature.

* Corresponding author. E-mail: toshimichi_kamei@ajinomoto.com.
† Fermentation and Biotechnology Laboratories.
‡ Institute of Life Sciences.
§ Iwate University.

10.1021/je8004968 CCC: $40.75
Published on Web 11/18/2008

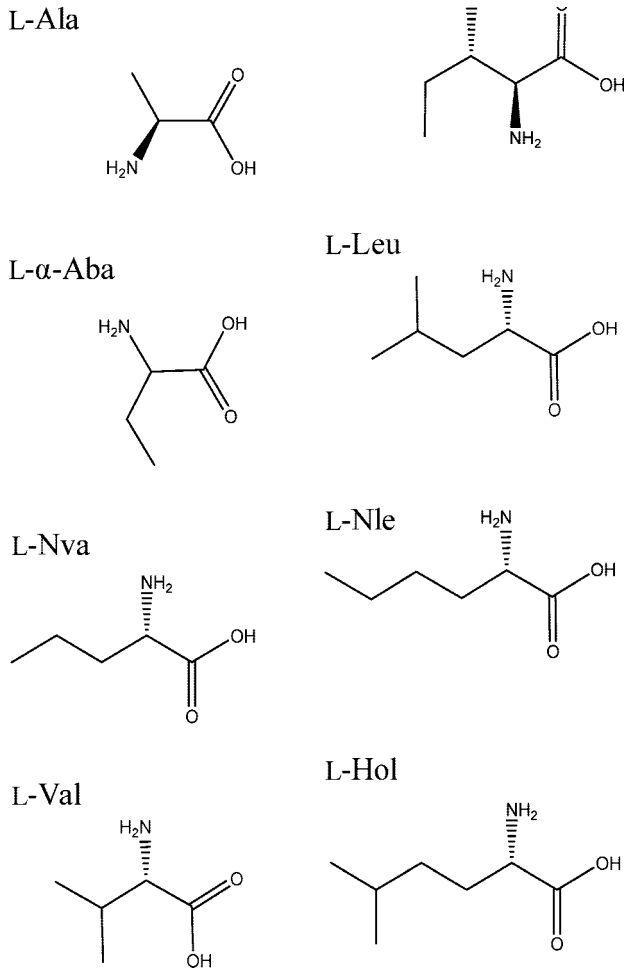

Figure 1. Molecular structures of BCAA and isomorphic amino acids. L-Alanine (L-Ala), L-isoleucine (L-Ile), L-leucine (L-Leu), L-norvaline (L-Nva), L-α-aminobutyric acid (L-α-Aba), L-norleucine (L-Nle), L-valine (L-Val), and L-homoleucine (L-Hol) are shown here.

Table 2. Compositions of the Starting Solutions and Corresponding Phases in Equilibrium in the L-Ile (1) + L-Ala (2) + Water (3) System at 293 K

	initial		equilibrium			
	liquid phase		liquid phase		solid phase	
run no.	$10^3\ x_1$	$10^3\ x_2$	$10^2\ x_1$	$10^2\ x_2$	x_1	x_2
run 1	2.74	0.00	0.46	0.00	1.00	0.00
run 2	2.75	0.14	0.46	0.05	0.99	0.01
run 3	2.74	0.54	0.45	0.23	0.97	0.03
run 4	2.74	1.08	0.44	0.52	0.95	0.05
run 5	2.74	1.61	0.43	0.70	0.93	0.07
run 6	2.73	2.15	0.42	0.92	0.91	0.09
run 7	2.73	4.02	0.39	1.97	0.84	0.16
run 8	2.73	5.36	0.35	2.47	0.80	0.20
run 9	2.73	6.69	0.36	2.91	0.77	0.23
run 10	3.61	8.00	0.35	2.85	0.74	0.26
run 11	1.45	8.00	0.35	2.86	0.22	0.78
run 12	1.09	8.01	0.34	2.86	0.13	0.87
run 13	0.91	8.03	0.36	2.97	0.07	0.93
run 14	0.54	8.02	0.27	2.92	0.00	1.00
run 15	0.36	8.02	0.18	2.81	0.00	1.00
run 16	0.18	8.02	0.10	2.81	0.00	1.00
run 17	0.00	8.02	0.00	2.97	0.00	1.00

Characterization of the washed crystals and the saturated liquor (mother liquor) was conducted in the same way as those made by Kamei et al.[3]

Results

Solid−Liquid Equilibria. The measured liquid compositions and solid compositions for the mixture L-Ile (1) + L-Ala (2) + water (3) are presented in Table 2 and are presented graphically in Figure 3. The liquid phase compositions were analyzed after achievement of steady state conditions. The steady state

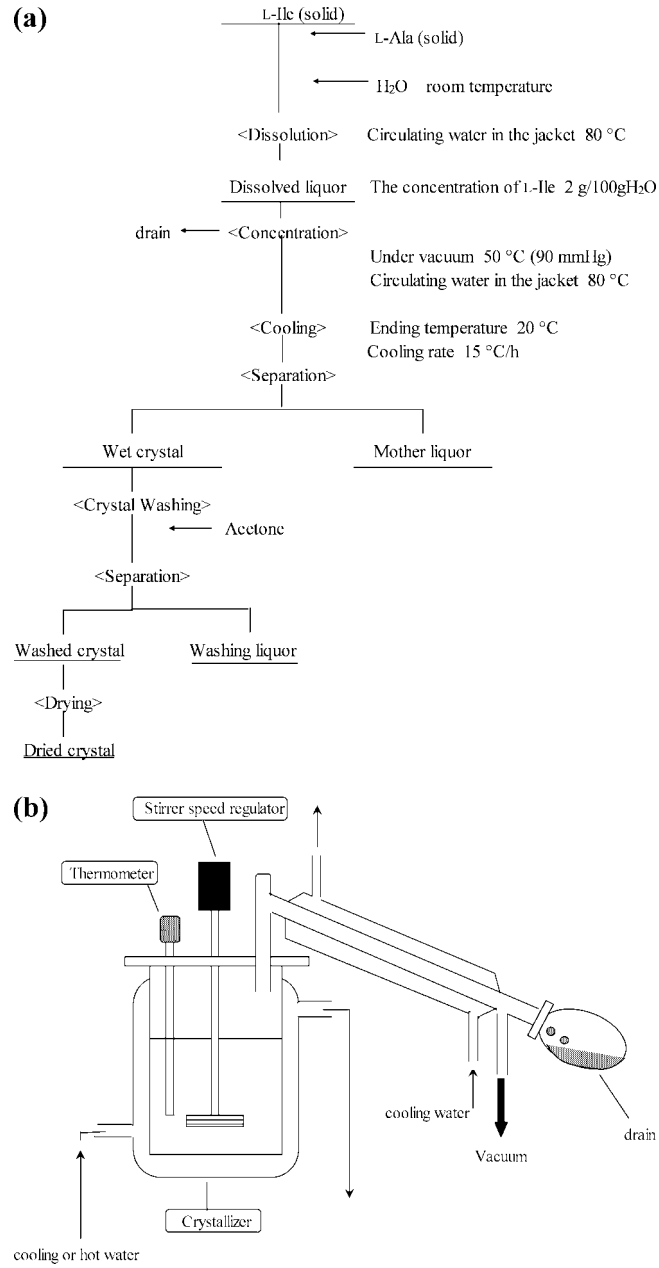

Figure 2. (a) Scheme of the crystallization method. (b) Experimental apparatus.

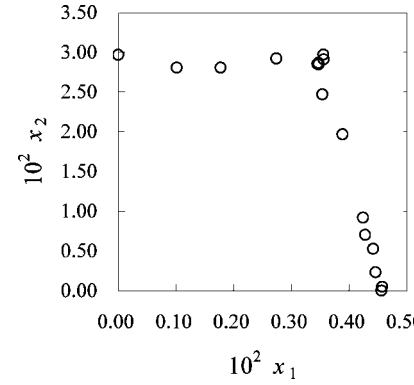

Figure 3. Ternary phase diagram for L-Ile (1) + L-Ala (2) + water (3). ○, Liquid phase composition.

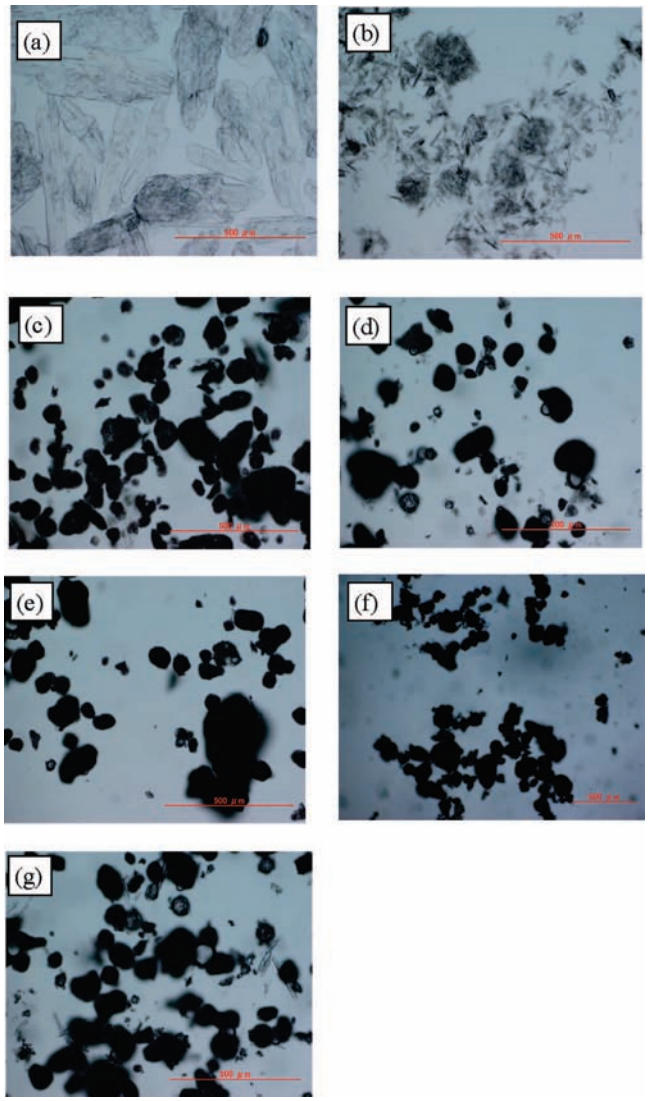

Figure 4. Change of the crystal appearance obtained by crystallization. (a) Run 1, L-Ile, pure. (b) Run 3, L-Ile + L-Ala (L-Ala mole fraction in crystals: 0.03). (c) Run 5, L-Ile + L-Ala (L-Ala mole fraction in crystals: 0.07). (d) Run 7, L-Ile + L-Ala (L-Ala mole fraction in crystals: 0.16). (e) Run 8, L-Ile + L-Ala (L-Ala mole fraction in crystals: 0.20). (f) Run 9, L-Ile + L-Ala (L-Ala mole fraction in crystals: 0.23). (g) Run 10, L-Ile + L-Ala (L-Ala mole fraction in crystals: 0.26) (redline scale: 500 μm).

conditions were verified by periodically withdrawing small samples of the liquid for analysis by an amino acid analyzer. Therefore, there were few experimental errors on the data, and an analysis error of the amino acid analyzer was controlled within 3 % in this experiment. Also, we confirmed the data from a mass balance in all cases.

Table 2 also lists the initial L-Ile mole fraction x_1 and L-Ala mole fraction x_2. The run number identifies the specific experiment. For example, in run 2, a homogeneous aqueous solution containing $x_1 = 2.75 \cdot 10^{-3}$ and $x_2 = 0.14 \cdot 10^{-3}$ was concentrated and cooled to obtain a liquid phase containing $x_1 = 0.46 \cdot 10^{-2}$ and $x_2 = 0.05 \cdot 10^{-2}$, in equilibrium with a solid phase containing $x_1 = 0.99$ and $x_2 = 0.01$. Pure L-Ile and pure L-Ala crystallization were conducted, respectively, in run 1 and run 17. As for run 1 and run 17, the composition of the liquid phase in equilibrium shows the aqueous solubility of the single component amino acid. According to literature values[11,12] and our previous work,[3] the compositions of the liquid phase of single L-Ile ((2*S*,3*S*)-2-amino-3-pentanoic acid) is $0.46 \cdot 10^{-2}$ (= x_1) at 19 °C[12] and $0.47 \cdot 10^{-2}$ (= x_1) at 20 °C,[3] respectively.

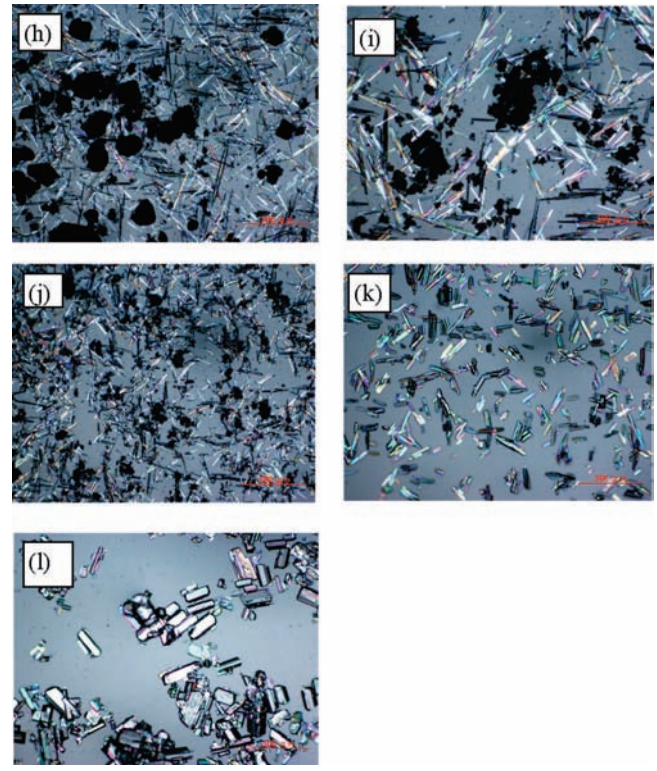

Figure 5. Change of the crystal appearance obtained by crystallization. (h) Run 11, L-Ile + L-Ala (L-Ala mole fraction in crystals: 0.78). (i) Run 12, L-Ile + L-Ala (L-Ala mole fraction in crystals: 0.87). (j) Run 13, L-Ile + L-Ala (L-Ala mole fraction in crystals: 0.93). (k) Run 14, L-Ala (L-Ala mole fraction in crystals: 1.00). (l) Run 17, L-Ala, pure, (redline scale: 500 μm).

Table 3. XRD Data and Calculated d-Spacing of Crystals of L-Ile (1) + L-Ala (2) Obtained in the Experiments Using Synchrotron X-Ray Diffraction Analysis[a]

		around the (001) face of L-Ile		around the (120) face of L-Ala	
run no.	solid phase x_1	peak position (2θ)	d-spacing d/Å	peak position (2θ)	d-spacing d/Å
run 1	1.00	4.10	13.99	-	-
run 3	0.97	4.10	13.99	-	-
run 5	0.93	4.10	13.99	-	-
run 7	0.84	4.11	13.93	-	-
run 8	0.80	4.13	13.93	13.29	4.32
run 9	0.77	4.13	13.93	13.29	4.32
run 10	0.74	4.13	13.93	13.29	4.32
run 11	0.22	4.13	13.93	13.29	4.32
run 12	0.13	4.13	13.93	13.29	4.32
run 13	0.07	4.13	13.93	13.29	4.32
run 14	0.00	-	-	13.29	4.32
run 17	0.00	-	-	13.31	4.32

[a] Wavelength = 1.0000 Å; peak region: around the (001) face of L-Ile and around the (120) face of L-Ala.

Also, the compositions of the liquid phase of single L-Ala ((*S*)-2-aminopropionic acid) is $3.09 \cdot 10^{-2}$ (= x_2) at 20 °C.[11] As shown in Table 2, in run 1, x_1 equals $0.46 \cdot 10^{-2}$ and in run 17 x_2 equals $2.97 \cdot 10^{-2}$, respectively. Therefore, the data measured in this work are in good agreement with literature values.

Table 2 and Figure 3 show that from run 2 to run 8 the L-Ile solubility decreases gradually with the increased mole fraction of L-Ala. From run 9 to run 13, although the compositions of the solid phases are different, the compositions of the liquid phases remain constant. From run 14 to run 16, the L-Ala solubility is not affected by the presence of L-Ile, and the solid phases do not contain L-Ile. The composition of the liquid phase

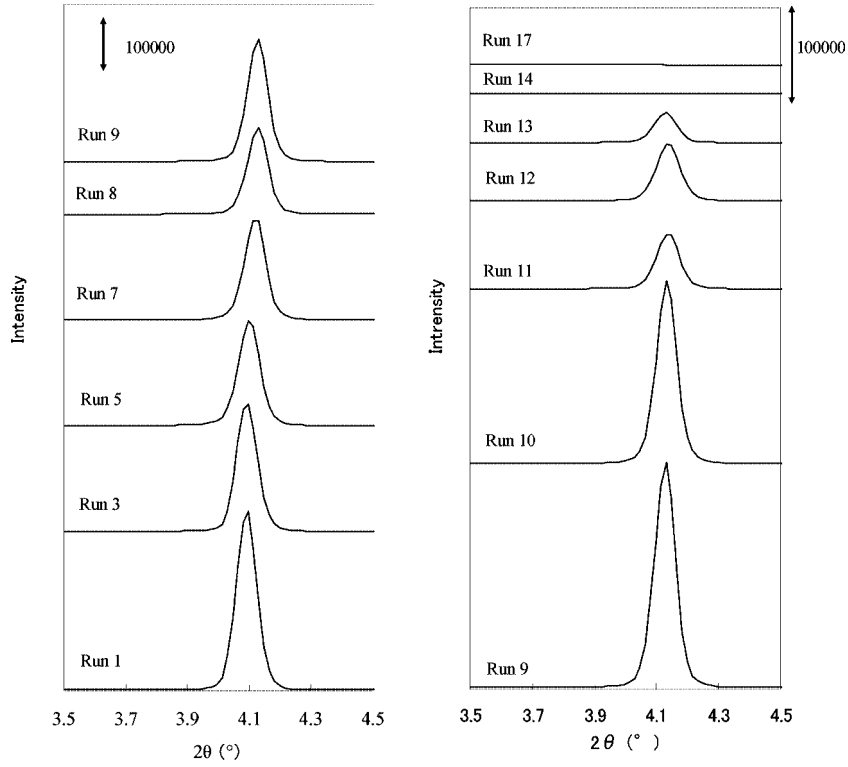

Figure 6. Powder XRD patterns of L-Ile + L-Ala crystals obtained in the experiments using synchrotron X-ray diffraction analysis (wavelength = 1.0000 Å, peak region: around the (001) face of L-Ile).

would remain constant if the solid phase were a mixture of pure L-Ile and pure L-Ala. Consequently, from run 2 to run 8, the possibility exists that the solid phase is not a mixture of pure L-Ile and pure L-Ala, but a solid solution is formed. In addition, from run 14 to run 16, even if L-Ile coexists in the solution, only L-Ala crystallized. Demonstrably, L-Ile is not incorporated in L-Ala in these runs.

Crystal Appearance. The solid phase appearances were observed to investigate the solid phase in run 9 to run 13. Representative cases are portrayed in Figures 4 and 5. Except for run 1 and run 17 (pure L-Ile and pure L-Ala), the appearances of the solid phase are classifiable into three categories. From run 1 to run 10, it gradually changes to a thick granular structure (Figure 4). From run 11 to run 13, the solid phases are mixtures of thick granular crystals and needle-like crystals (Figure 5). In addition, from run 14 to run 16, only needle-like crystals are observed (Figure 5); it is considered that these crystals are L-Ala. Therefore, from run 9 to run 13, the possibility exists that the solid phases gradually change from homogeneous substances to inhomogeneous mixtures including at least two phases.

XRD Pattern. Figures 6 and 7 depict powder XRD diffraction patterns of representative crystals obtained from experiments using synchrotron X-ray diffraction analysis (wavelength = 1.0000 Å).

Actually, L-Ile is monoclinic and belongs to the $P2_1$ space group.[8] In addition, the peak of the highest intensity corresponds to the (001) face at 4.1° (wavelength = 1.0000 Å). The L-Ala is orthorhombic and belongs to the $P2_12_12_1$ space group.[10] Its highest intensity peak corresponds to the (120) face at 13.3° (wavelength = 1.0000 Å). Therefore, to identify solid phases, these peaks were confirmed. Figure 6 and Table 3 show the XRD peak around the (001) face of L-Ile. By using synchrotron radiation, we could obtain the XRD pattern with an extraordinarily high degree of accuracy. In this case, the range of error on the peak positions and d-spacing were confirmed below 0.01° and below 0.04 Å by using a silicon standard. From run 1 to run 8, as the L-Ala composition in the solid phase increases, the XRD peak in the (001) face of L-Ile slightly shifts from 4.10° to 4.13°. On the other hand, this peak does not shift from run 8 to run 13 at 4.13°. This peak disappears after run 14.

Figure 7 and Table 3 show the XRD peak around the (120) face of L-Ala. From run 8, the peak of the (120) face of L-Ala clearly appeared. This peak does not shift from run 8 to run 13. Therefore, L-Ala exists from run 8 to run 13. Additionally, as for Figure 7, pure L-Ile (run 1) and pure L-Ala (run 17) have the same XRD peak at 14.5°. This peak corresponds to the (112) face of L-Ile and the (111) face of L-Ala, and the peak scale was suitable for describing the change of XRD pattern in this case. The peak intensity depends on the sample condition. For example, sample orientation might effect the peak intensity. Therefore, the peak intensity is rather qualitative.

As another feature, the following phenomenon was observed. In this experiment, XRD profiles were obtained from the 0° to 40° angle. Within this observed range, we found that the new XRD peak (around 12.5°) gradually appears with increased mole fraction of L-Ala (Figure 8). Furthermore, this peak disappears after run 14. In addition, this peak does not correspond to pure L-Ile and L-Ala peaks. Therefore, it is considered that a new phase appears from run 2 to run 13.

A solid solution exists from run 2 to run 13. In addition, pure L-Ala coexists with a solid solution from run 8 to run 13. From run 8 to run 13, the phase composition of a solid solution is the same from the XRD result, but the amount of coexisting pure L-Ala is different. The solid phase compositions in Table 2 were overall compositions of pure L-Ala and a solid solution. Then, from run 14, only pure L-Ala exists in the solid phase. Especially from run 8 to run 13, it is considered that a solid solution crystallizes first. Then pure L-Ala beyond the L-Ala solubility crystallizes.

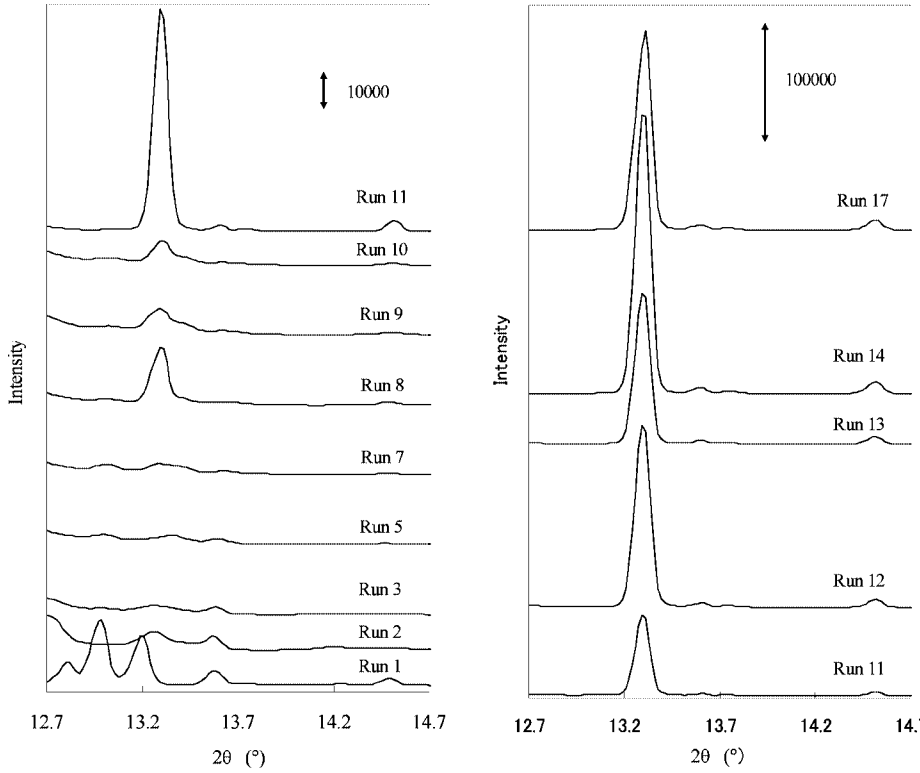

Figure 7. Powder XRD patterns of L-Ile + L-Ala crystals obtained in the experiments using synchrotron X-ray diffraction analysis (wavelength = 1.0000 Å, peak region: around the (120) face of L-Ala).

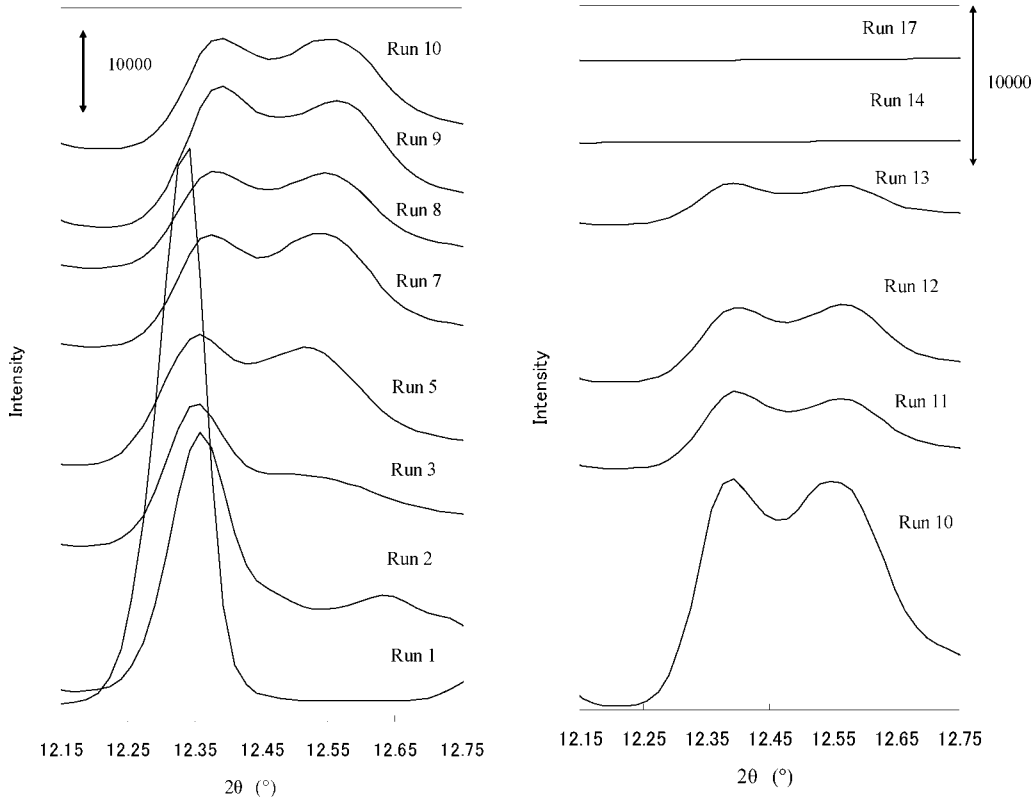

Figure 8. Powder XRD patterns of L-Ile + L-Ala crystals obtained in the experiments using synchrotron X-ray diffraction analysis (wavelength = 1.0000 Å, peak region: around $2\theta = 12.5°$).

Conclusion

The L-Ile solubility decreased gradually with increased mole fraction of L-Ala when x_1 (mole fraction of L-Ile) in the solid phase is 0.99 to 0.80 (in run 2 to run 8). However, the L-Ala solubility was not affected by the presence of a small amount of L-Ile. In addition, when x_1 in the solid phase is 0.80 to 0.07 (in run 8 to run 13), the compositions of the liquid phases remain constant although the compositions of the solid phases differ

because the phase composition of a solid solution is the same in run 8 to run 13.

As for the solid phase, the existing states are considered as follows.

The L-Ile and L-Ala form a solid solution uniformly when x_1 in the solid phase is 0.99 to 0.80 (in run 2 to run 8). On the other hand, when x_1 in the solid phase is 0.80 to 0.07 (in run 8 to run 13), the solid phases change from a homogeneous solid solution to inhomogeneous mixtures of pure L-Ala and a solid solution. In addition, from run 14 to run 16, the solid phase is only pure L-Ala. This result differs from that described in previous reports, which showed the formation of a solid solution in all compositions.

Acknowledgment

Powder X-ray diffraction analysis was conducted using the synchrotron radiation at the Pharmaceutical Industry Beamline BL32B2 in the SPring-8 with the approval of the Japan Synchrotron Radiation Research Institute (JASRI) (Proposal No. 2008A5962).

Literature Cited

(1) Toshimichi, K.; Kazuhiro, H.; Ichiro, F.; Hidetada, N.; Masaaki, Y.; Norihito, D.; Kenji, S. Mechanism of Mutual Incorporation of Branched Chain Amino Acids and Isomorphic Amino Acids in Batch Crystallization. *J. Chem. Eng. Jpn.* **2008**, *41*, 460–469.

(2) Toshimichi, K.; Kazuhiro, H.; Tatuki, K.; Eiichiro, S.; Masaaki, Y.; Norihito, D.; Kenji, S. Mechanism of Mutual Incorporation of L-Isoleucine and Isomorphic Amino Acids in Batch Crystallization. *Org. Process Res. Dev.* **2008**, *12*, 850–854.

(3) Toshimichi, K.; Kazuhiro, H.; Tatuki, K.; Eiichiro, S.; Masaaki, Y.; Norihito, D.; Kenji, S. Solid−Liquid equilibria in an L-Isoleucine + L-Norleucine + Water System. *J. Chem. Eng. Data* **2008**, *53*, 1338–1341.

(4) Kurosawa, I.; Amyn, S. T.; Ronald, W. R. Solid-liquid equilibria in L-leucine + L-valine + water. *Fluid Phase Equilib.* **2004**, *224*, 245–249.

(5) Kurosawa, I.; Amyn, S. T.; Ronald, W. R. Solubility Measurements in the L-Isoleucine + L-Valine + Water System at 298 K. *Ind. Eng. Chem. Res.* **2005**, *44*, 3284–3288.

(6) Harding, M. M.; Howieson, R. M. L-Leucine. *Acta Cryst. B* **1976**, *32*, 633–634.

(7) Torii, K.; Iitaka, Y. The Crystal Structure of L-Valine. *Acta Cryst. B* **1970**, *26*, 1317–1326.

(8) Torii, K.; Iitaka, Y. The Crystal Structure of L-Isoleucine. *Acta Cryst. B* **1971**, *27*, 2237–2246.

(9) Torii, K.; Iitaka, Y. Crystal Structures and Molecular Conformations of L-Methionie and L-Norleucine. *Acta Cryst. B* **1973**, *29*, 2799–2807.

(10) Harry, J. S.; Richard, E. M. The Crystal Structure of L-Alanine. *Acta Crystallogr.* **1966**, *20*, 550–555.

(11) Peijun, J.; Wei, F. Solubility Of Amino Acids In Water And Aqueous Solutions By the Statistical Associating Fluid Theory. *Ind. Eng. Chem. Res.* **2008**, *47*, 6275–6279.

(12) Jeffrey, C. G.; Amyn, S. T.; Ronald, W. R. Effect of Relative Solubility on Amino Acid Crystal Purity. *AIChE J.* **2001**, *47*, 2705–2712.

Received for review June 30, 2008. Accepted October 18, 2008.

JE8004968